

# Molecular Motion in Liquids: The Partially Rigid Molecule 1,2,3,4-Tetrahydro-5,6-Dimethyl-1,4-Methanonaphthalene. Temperature Dependence of $^{13}\text{C}$ Magnetic Relaxation and Correlation Times

U. Schlenz\*, A. Dölle\*\*, and H. G. Hertz\*

\* Institut für Physikalische Chemie und Elektrochemie, Universität Karlsruhe, Kaiserstraße 12, D-76128 Karlsruhe

\*\* Institut für Physikalische Chemie, Rheinisch-Westfälische Technische Hochschule, Templergraben 59, D-52056 Aachen

Z. Naturforsch. **50a**, 631–642 (1995); received December 16, 1994

*Dedicated to Professor W. Müller-Warmuth on occasion of his 65th birthday*

For the hydrocarbon 1,2,3,4-tetrahydro-5,6-dimethyl-1,4-methanonaphthalene (5,6-Me<sub>2</sub>-THMN)  $^{13}\text{C}$  longitudinal relaxation times and NOE factors were measured over a wide temperature range at frequencies of 22.63 and 100.62 MHz. Additionally,  $^{13}\text{C}$  transversal relaxation times were measured at 100.62 MHz. The relaxation data show that the dispersion region is already reached at moderate temperatures. The experimental data were modeled by the combination of the Vogel-Fulcher-Tammann ansatz and a scaling of the dipolar coupling constant with a factor of 0.70. From the fit of the data also activation parameters of the rotational motion of the molecules were obtained. Although the molecules of 5,6-Me<sub>2</sub>-THMN have a rigid structure (except the two internally rotating methyl groups), the model of the rotational diffusion of rigid bodies does not satisfactorily describe the relaxation data.

**Key words:** Liquids, Rotational Diffusion, Rotational Correlation Times,  $^{13}\text{C}$  Nuclear Magnetic Resonance, Relaxation.

## 1. Introduction

A quite frequently applied model for describing dynamics of molecules in liquids is that of diffusion including rotational motion. The measurement of nuclear relaxation data is a particularly important method for making statements about molecular dynamics. In case of  $^{13}\text{C}$  relaxation, the most prominent relaxation mechanism is that of dipolar interaction. The dipolar relaxation data are connected to molecular properties by the dipolar coupling constant and by the molecular reorientational correlation times *via* the spectral densities. Most of the experimental findings have been made in the extreme narrowing regime. In this region the product of correlation time and measuring frequency is much smaller than unity and the relaxation data are frequency independent. When the measurements are extended to the dispersion regime, the relaxation data depend on the measuring frequency and the condition of extreme narrowing is no longer fulfilled.

The interpretation of experimental data obtained in the dispersion regime often failed: With the assumption that rotating molecules behave as rigid bodies, it was frequently impossible to reproduce the experimentally observed relaxation data by calculation with the proposed models (cf. e.g. [1–4]). It is thus questionable whether the rotational diffusion model, as it is normally applied for determining the rotational dynamical parameters in liquids, is still applicable. One criterion for the condition of the rigid body is that the maximum value of the spectral density coincides for calculated and experimental values [1, 2]. When this criterion is not fulfilled, continuous distributions of correlation times of various types [5] can be used to correct for the missing spectral density. This was successful for interpreting relaxation data from organic molecules in simple organic glass-forming systems and zeolites by the Cole-Davidson distribution function [6, 7]. Another approach which implies discrete distributions of correlation times, is to assume the existence of further motional modes not considered by the usual models of rotational motions [1].

It was the aim of the present study to investigate again whether the model of rotational diffusion of

Reprint requests to Dr. A. Dölle.

0932-0784 / 95 / 0700-0631 \$ 06.00 © – Verlag der Zeitschrift für Naturforschung, D-72027 Tübingen



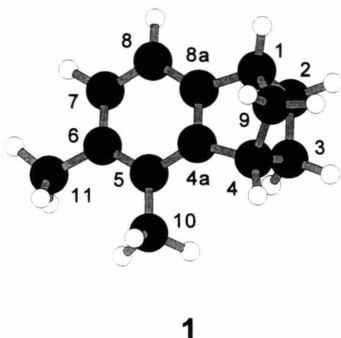
Dieses Werk wurde im Jahr 2013 vom Verlag Zeitschrift für Naturforschung in Zusammenarbeit mit der Max-Planck-Gesellschaft zur Förderung der Wissenschaften e.V. digitalisiert und unter folgender Lizenz veröffentlicht: Creative Commons Namensnennung-Keine Bearbeitung 3.0 Deutschland Lizenz.

Zum 01.01.2015 ist eine Anpassung der Lizenzbedingungen (Entfall der Creative Commons Lizenzbedingung „Keine Bearbeitung“) beabsichtigt, um eine Nachnutzung auch im Rahmen zukünftiger wissenschaftlicher Nutzungsformen zu ermöglichen.

This work has been digitalized and published in 2013 by Verlag Zeitschrift für Naturforschung in cooperation with the Max Planck Society for the Advancement of Science under a Creative Commons Attribution-NoDerivs 3.0 Germany License.

On 01.01.2015 it is planned to change the License Conditions (the removal of the Creative Commons License condition “no derivative works”). This is to allow reuse in the area of future scientific usage.

rigid bodies is appropriate for describing rotational motions of molecules in the liquid phase. For such a task a compound has to be studied which mainly contains rigid structural units, for which rotational motion is slow enough at moderate temperatures, and which has enough different nuclei for which relaxation data can be obtained.



All of these requirements are met by the model compound 5,6-dimethyl-1,2,3,4-tetrahydro-1,4-methanonaphthalene (5,6-Me<sub>2</sub>-THMN, **1**) [8]. The neat hydrocarbon **1** is liquid at ambient temperature and shows only a glass transition at 188 K ( $1000/T_g = 5.32 \text{ K}^{-1}$ ) [9]. The main part of it, namely the aromatic ring and the condensed cyclopentane unit, is rigid. In [10] (part 2 of the series) the molecules of **1** were assumed to be rigid when describing their rotational motions in the neat liquid and in the extreme narrowing regime. In the present study it was investigated whether this assumption really holds in the dispersion region. For that purpose the  $^{13}\text{C}$  relaxation data of **1** were measured in and below the extreme narrowing regime, and a first and somewhat preliminary approach was attempted to fit the experimental data with simple models for rotational dynamics.

## 2. Experimental

The measurements were carried out under broad-band  $^1\text{H}$  decoupling on Bruker WH 90 ( $B_0 = 2.114 \text{ T}$ ,  $\nu_0(^{13}\text{C}) = 22.63 \text{ MHz}$ ,  $\nu_0(^1\text{H}) = 90.055 \text{ MHz}$ ) and AM 400 ( $B_0 = 9.395 \text{ T}$ ,  $\nu_0(^{13}\text{C}) = 100.62 \text{ MHz}$ ,  $\nu_0(^1\text{H}) = 400.13 \text{ MHz}$ ) spectrometers. Longitudinal relaxation times and NOE factors were extracted from signal heights, and the transversal relaxation times from the line widths at half height after correction for inhomogeneity broadening of the resonances. The  $^{13}\text{C}$

spin-lattice relaxation times were obtained by a three parameter exponential fit implemented in the spectrometer software. An exception was the spin-lattice relaxation of the methyl carbons which showed a biexponential decay of the magnetization in the temperature range around the maximum of the longitudinal relaxation rate. The relaxation times were calculated here from the initial decay rate of the magnetization with a formalism by Pöschl *et al.* [11]. Temperatures were determined before and after measurements of the relaxation data on the AM 400 spectrometer by temperature-dependent  $^1\text{H}$  chemical-shift measurements [12] of neat 1,2-ethanediol or methanol, and for the WH 90 spectrometer by a Pt-100 resistance thermometer; for the latter temperature measurements the broad-band decoupler was shortly switched off. The error in the temperature was estimated to be  $\pm 1 \text{ K}$ .

The mean standard deviations of the mean values for the experimental data were below 1% in most cases. However, the “real” error for the relaxation times is believed to lie between  $\pm 3$  and  $\pm 5\%$ , for the relaxation times from biexponential data at about  $\pm 5\%$ , and for the NOE factors at less than 10%. Further details concerning experimental techniques and sample preparation are given in [8, 21].

Data evaluation was performed with the aid of FORTRAN 77 programs which performed a  $\chi^2$  fit of the model parameters to the experimental relaxation data by the Levenberg-Marquardt method [13]. In order to obtain reasonable values for the  $\chi^2$  test and for the standard deviations of the fitted parameters, a mean standard deviation of 3% for the spin-lattice relaxation times at 100.62 MHz and of 5% for all other experimental data was assumed. The bond distance information was obtained from a geometry optimization using the AM1 method [14] from the MOPAC package [15]. The following distances between the carbons and their directly bonded protons were obtained: for carbons C1 and C4 110.4 pm, C2 and C3 111.5 pm, C9 111.1 pm, C7 110.1 pm, C8 109.8 pm, C10 and C11 111.9 pm.

## 3. Theoretical Background

The longitudinal or transversal nuclear relaxation rates observed in NMR experiments,  $1/T_1$  or  $1/T_2$ , respectively, are given as the sum over the rates of the contributions from the different relaxation mechanisms, with the assumption that cross terms can be

neglected. For measuring  $^{13}\text{C}$  relaxation rates with decoupling the  $^{13}\text{C}$  nuclei from the protons, also the term for cross relaxation vanishes [16]. When discussing the contributions of the various relaxation mechanisms [16] to the  $^{13}\text{C}$  relaxation of **1**, besides the dipolar mechanism (DD) only relaxation by spin rotation (SR) interaction and chemical-shift anisotropy (CSA) has to be taken into account. While relaxation *via* the SR mechanism increases with rising temperature, relaxation by CSA has the same temperature dependence in the extreme narrowing region as the DD mechanism. The importance of the CSA relaxation increases quadratically with the magnetic field strength of the static field.

With the simplifying assumption of isotropic re-orientation the dipolar relaxation rates  $(1/T_1)_i$  and  $(1/T_2)_i$  for relaxation of a  $^{13}\text{C}$  nucleus  $i$  by  $n_{\text{H}}$  protons  $j$  is connected to the molecular rotations by the equations [16]

$$\left(\frac{1}{T_1^{\text{DD}}}\right)_i = \frac{1}{10} \left(\frac{\mu_0}{4\pi}\right)^2 \frac{\gamma_{\text{C}}^2 \gamma_{\text{H}}^2 \hbar^2 n_{\text{H}}}{r_{ij}^6} \cdot (J(\omega_{\text{H}} - \omega_{\text{C}}) + 3J(\omega_{\text{C}}) + 6J(\omega_{\text{H}} + \omega_{\text{C}})) \quad (1)$$

and

$$\left(\frac{1}{T_2^{\text{DD}}}\right)_i = \frac{1}{10} \left(\frac{\mu_0}{4\pi}\right)^2 \frac{\gamma_{\text{C}}^2 \gamma_{\text{H}}^2 \hbar^2 n_{\text{H}}}{r_{ij}^6} \cdot \left(2J(0) + \frac{1}{2}J(\omega_{\text{H}} - \omega_{\text{C}}) + \frac{3}{2}J(\omega_{\text{C}}) + 3J(\omega_{\text{H}}) + 3J(\omega_{\text{H}} + \omega_{\text{C}})\right) \quad (2)$$

with  $\mu_0$  the permeability constant of the vacuum,  $\gamma_{\text{C}}$  and  $\gamma_{\text{H}}$  the gyromagnetic ratios of  $^{13}\text{C}$  and  $^1\text{H}$ , respectively,  $r_{ij}$  the length of the internuclear vector between  $i$  and  $j$ , and  $J(\omega)$  the spectral density at frequency  $\omega$ . The NOE factor  $\eta_i$  of carbon atom  $i$  for relaxation by  $n$  protons  $j$  is obtained as [16, 17]

$$\eta_i = \frac{\gamma_{\text{H}} \sum_{j=1}^n \sigma_{ij}}{\gamma_{\text{C}} \sum_{j=1}^n \varrho_{ij} + \varrho_i^*}, \quad (3)$$

where  $\sigma_{ij}$  is the cross relaxation rate,  $\varrho_{ij}$  the direct dipolar relaxation rate, and  $\varrho_i^*$  the so-called leakage term which represents the contribution of all other relaxation mechanisms to the relaxation of atom  $i$  and which reduces the Overhauser factor. The sum of  $\varrho_{ij}$  over all  $n_{\text{H}}$  interacting protons gives under  $^1\text{H}$  decou-

pling the dipolar spin-lattice relaxation rate  $1/T_1^{\text{DD}}$ . For the relaxation of  $^{13}\text{C}$  exclusively *via* the dipolar interaction,  $\varrho_i^* = 0$ , the NOE factor reaches maximum and depends only on the molecular dynamics with [16, 17]

$$\eta_{i,\text{max}} = \frac{\gamma_{\text{H}}}{\gamma_{\text{C}}} \cdot \frac{6J(\omega_{\text{H}} + \omega_{\text{C}}) - J(\omega_{\text{H}} - \omega_{\text{C}})}{J(\omega_{\text{H}} - \omega_{\text{C}}) + 3J(\omega_{\text{C}}) + 6J(\omega_{\text{H}} + \omega_{\text{C}})}. \quad (4)$$

The spectral densities are obtained by Fourier transformation of the corresponding molecular rotational time correlation functions. When the rotational motions are characterized by a single correlation time  $\tau_{\text{c}}$ , the spectral density is

$$J(\omega) = \frac{\tau_{\text{c}}}{1 + (\omega \tau_{\text{c}})^2}. \quad (5)$$

For modeling the rotational dynamics of viscous liquids, glasses and solids the Cole-Davidson (CD) distribution function of correlation times [6] often describes the experimental data better. Its spectral density function is given by

$$J(\omega) = \frac{\sin(\beta \arctan(\omega \tau_{\text{CD}}))}{\omega(1 + (\omega \tau_{\text{CD}})^2)^{\beta/2}} \quad (6a)$$

and [5]

$$J(0) = \beta \tau_{\text{CD}}, \quad (6b)$$

where  $\tau_{\text{CD}}$  denotes the maximum correlation time, i.e. the cut-off of the distribution function, and  $\beta$  is the width of the distribution.

Since it is normally not possible to measure relaxation data at enough different frequencies and calculate the spectral density as a frequency-dependent quantity, the temperature is chosen as the independent variable. The temperature dependence of the molecular correlation times in liquids is usually represented by the Arrhenius ansatz

$$\tau_{\text{c}} = \tau_0 \exp\left(\frac{E_{\text{A}}}{RT}\right). \quad (7)$$

In viscous liquids and in glasses the activation energy  $E_{\text{A}}$  appears to grow with decreasing temperature. This finding is phenomenologically described by the Vogel-Fulcher-Tammann (VFT) ansatz [18–20]

$$\tau_{\text{c}} = \tau_0 \exp\left(\frac{E_{\text{VFT}}}{R(T - T_0)}\right). \quad (8)$$

The parameter  $T_0$  is of the order of magnitude of the glass temperature  $T_g$ .

The spin-lattice relaxation dispersion curve at fixed measuring frequencies is determined by two parameters: the slope of the relaxation function ( $\ln(1/T_1) = f(1/T)$ ) and the height of its maximum. The latter is given for dipolar relaxation by the dipolar coupling constant which is determined by the internuclear distance  $r_{ij}$  between the carbon  $i$  and the interacting protons  $j$ . The absolute value of the slope of the longitudinal relaxation function is partly characterized by an activation energy, and in case of the VFT ansatz also by  $T_0$ . When the distance between the interacting nuclei is known, the dipolar coupling constant can be calculated. From NMR relaxation experiments, however, often a coupling constant is obtained which appears to be too low when compared to the calculated value. In order to take this fact into account, the dipolar coupling constant in (1) can be scaled down by a constant factor  $C$ :

$$\left(\frac{1}{T_1^{\text{DD}}}\right)_i = C \frac{1}{10} \left(\frac{\mu_0}{4\pi}\right)^2 \frac{\gamma_C^2 \gamma_H^2 \hbar^2 n_H}{r_{ij}^6} \cdot (J(\omega_H - \omega_C) + 3J(\omega_C) + 6J(\omega_H + \omega_C)). \quad (9)$$

This has the physical meaning of stating that modes of faster molecular motion exist for which, however, further specification is lacking. In this regard it is particularly useful to treat the relaxation data with the CD distribution of the correlation times, as the maximum height is lowered with decreasing parameter  $\beta$ . Thus, at least formally, the fast motion is specified as part of the correlation function.

The temperature dependence of the NOE factors is not at all determined by the dipolar coupling constant and reflects just the dynamics of the dipole-dipole interaction.

## 4. Results

### 4.1 $^{13}\text{C}$ Relaxation Times and NOE Factors [21]

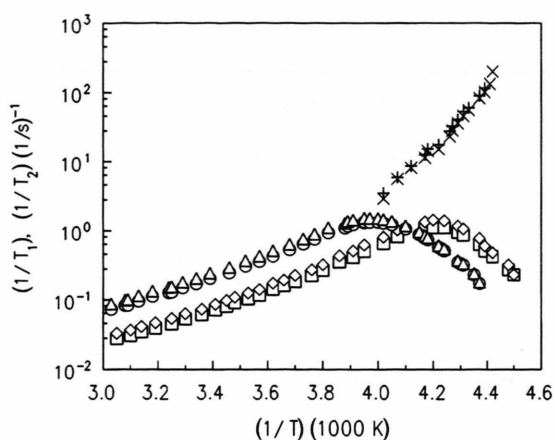
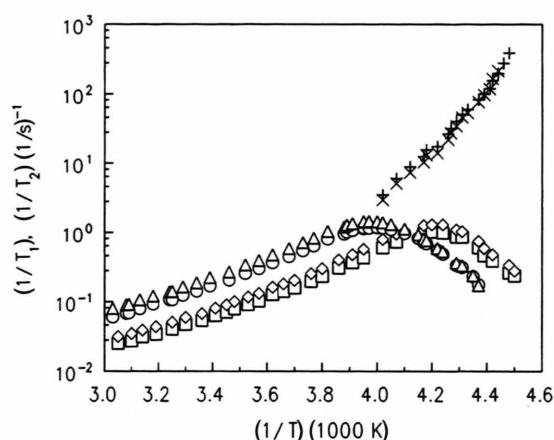
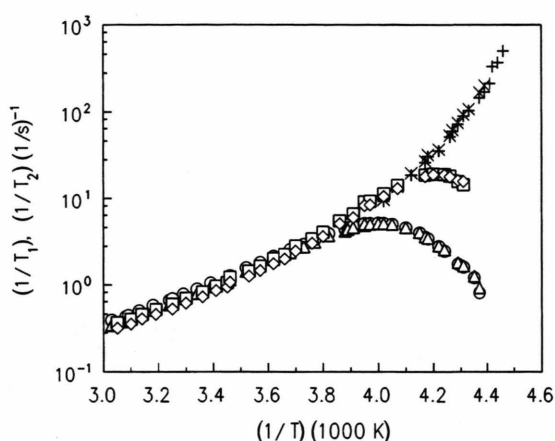
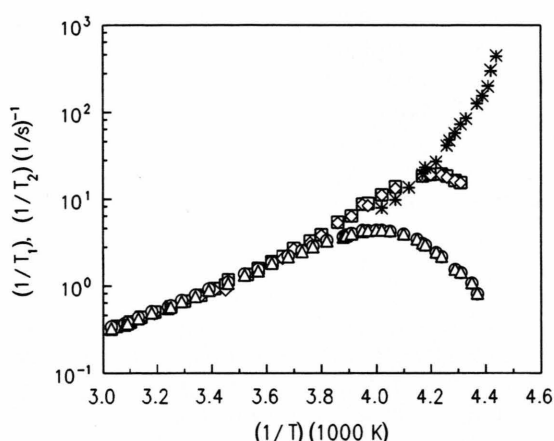
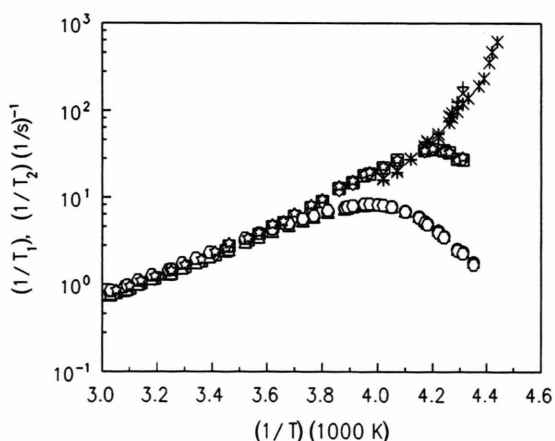
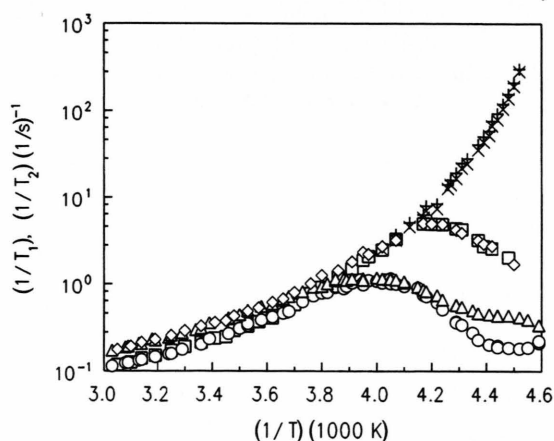
$^{13}\text{C}$  spin-lattice relaxation times  $T_1$  of neat 5,6-Me<sub>2</sub>-THMN were measured at 22.63 MHz in a temperature range from 222 to 328 K, at 100.62 MHz from 218 to 330 K, and transversal relaxation times at 100.62 MHz from 221 to 249 K. The observed relaxation rates  $(1/T_1)_{\text{exp}}$  and  $(1/T_2)_{\text{exp}}$  are presented in Fig. 1 as functions of  $1/T$ . They increase at first with increasing reciprocal temperature. This behavior is

caused by a decrease in the rate of molecular reorientation which results in an increase of the correlation times for the corresponding molecular rotations. The absolute value of the slope of the relaxation rates increases with increasing reciprocal temperature. With further increase of the reciprocal temperature a maximum of the longitudinal relaxation rate is reached: The temperature for the maximum is about 235 K at a measuring frequency of 22.63 MHz and about 250 K at 100.62 MHz. The relaxation curve is asymmetric, showing a more pronounced slope on the low temperature side of the maximum, which, in principle, is consistent with the VFT approach. On the other hand, the transverse relaxation rates show a monotonical increase with reciprocal temperature.

The measured values for the longitudinal relaxation rates in the extreme narrowing regime are equal for the corresponding methine and methylene carbon atoms of the non-aromatic carbons at the two measuring frequencies within the experimental error (Figs. 1 D to 1 F). The relaxation rates of the aromatic  $^{13}\text{C}$  nuclei are higher at 100.62 MHz because of the larger CSA contribution to relaxation (Figs. 1 A to 1 C).

The relaxation rates of the methyl  $^{13}\text{C}$  nuclei divided by the number  $n_H$  of directly bonded protons are smaller for all temperatures than the respective values for the methine and methylene carbons by a factor of about 10. This value is just the value of  $(1/4)(3\cos^2(\vartheta) - 1)^2 \approx 0.098$  for a methyl group undergoing rotational motions much faster than the overall rotational dynamics of the molecule [1] with  $\vartheta$  as the angle which the C–H vector forms with the axis of internal rotation; in the case of compound 1  $\vartheta = 110.63^\circ$ . This is an interesting observation, because in most cases so far known the angular relations demanded by the Woessner theory [22, 23] could not be demonstrated to be fulfilled [1–4, 24–26]. Here, since the factor  $(1/4)(3\cos^2(\vartheta) - 1)^2$  is deduced from the Woessner theory, at least one part of the corresponding requirements is fulfilled. At lower temperatures a larger second maximum having a height of  $(1 - (1/4)(3\cos^2(\vartheta) - 1)^2)(3/n_H)(1/T_1(\text{CH}_n))_{\text{exp}}$  compared to that of an aliphatic methine ( $n_H = 1$ ) or methylene ( $n_H = 2$ ) carbon nucleus is expected. However, with the experimental facilities used in the present investigation this temperature range was not accessible. Furthermore, the spin-lattice relaxation rates of the methyl carbon atoms (Fig. 1 F) for 100.62 MHz at about  $4.5 \cdot 10^{-3} \text{ K}^{-1}$  show a shoulder (C11) or a minimum (C10), respectively, the latter indicating already the increase of the relaxation



A) Quaternary aromatic carbon atoms 4a ( $\square$ ,  $\circ$ ,  $\times$ ) and 8a ( $\diamond$ ,  $\Delta$ ,  $+$ ).B) Quaternary aromatic carbon atoms 5 ( $\square$ ,  $\circ$ ,  $\times$ ) and 6 ( $\diamond$ ,  $\Delta$ ,  $+$ ).C) Methine aromatic carbon atoms 7 ( $\square$ ,  $\circ$ ,  $\times$ ) and 8 ( $\diamond$ ,  $\Delta$ ,  $+$ ).D) Methine aliphatic carbon atoms 1 ( $\square$ ,  $\circ$ ,  $\times$ ) and 4 ( $\diamond$ ,  $\Delta$ ,  $+$ ).E) Methylene aliphatic carbon atoms 2 ( $\square$ ,  $\circ$ ,  $\times$ ), 3 ( $\diamond$ ,  $\Delta$ ,  $+$ ), and 9 ( $\ast$ ,  $\circ$ ,  $\ast$ ).F) Methyl carbon atoms 10 ( $\square$ ,  $\circ$ ,  $\times$ ) and 11 ( $\diamond$ ,  $\Delta$ ,  $+$ ).Fig. 1. Experimental  $^{13}\text{C}$  longitudinal relaxation rates  $1/T_1$  at 22.63 MHz ( $\square$ ,  $\diamond$ ,  $\ast$ ) and 100.62 MHz ( $\circ$ ,  $\Delta$ ,  $\circ$ ) and transversal relaxation rates  $1/T_2$  at 100.62 MHz ( $\times$ ,  $+$ ,  $\ast$ ).

rates to form the second maximum. The shoulder is an interesting feature about which, however, at present no further information can be given.

In Fig. 2 the nuclear Overhauser factors (NOE)  $\eta$  are plotted against  $1/T$ . They were measured at 22.63 MHz from 223 to 328 K and at 100.62 MHz from 232 to 323 K. Within the experimental error the maximum NOE factor of 1.988 in the extreme narrowing regime was obtained for all  $^{13}\text{C}$  nuclei with directly bonded protons in the rigid molecular frame. The only exceptions are the aromatic methine  $^{13}\text{C}$  nuclei 7 and 8 at a measuring frequency of 100.62 MHz. Thus, in the former case the measured relaxation times are equal to the dipolar ones. Above a temperature of about 298 K the NOE factors of the  $^{13}\text{C}$  nuclei 10 and 11 in the methyl groups drop to a value below the maximum  $\eta$  for both measuring frequencies. For the methyl carbons and temperatures below 298 K the dipolar longitudinal relaxation times were equated with the observed ones.

As can be seen in Figs. 2A to 2E, the NOE factors of the non-methyl  $^{13}\text{C}$  nuclei were constant at high temperatures and then decreased quickly at lower temperatures. A continuous decrease of the NOE factors in the extreme narrowing regime with rising temperatures can only result from an increase of the spin rotation contribution. Thus, the temperature dependence of the NOE factors at lower temperatures is due to the fact that the condition of extreme narrowing was no longer fulfilled. The NOE factors of the aromatic carbon atoms in the extreme narrowing region deviated from the maximum value of 1.988 because of relaxation *via* the CSA mechanism (Figs. 2A to 2C), which was confirmed by the higher (or slightly higher, Fig. 1C) relaxation rates for the higher magnetic field strengths. The NOE factors of the methyl  $^{13}\text{C}$  nucleus of C10 (Fig. 2F) decreased in the extreme narrowing regime because of the growing contribution of the SR mechanism with increasing temperature. (Since the measuring error is too large, the situation is not so clear for C11). While  $\eta$  still reaches its maximum value for carbon atom 11, this is not the case for C10.

The assumed standard deviations in Figs. 1 and 2 are smaller or about the size of the symbols.

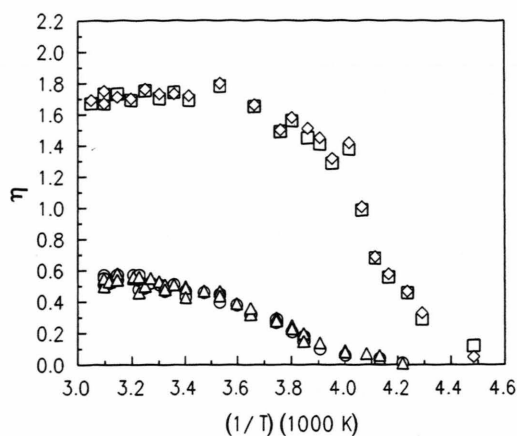
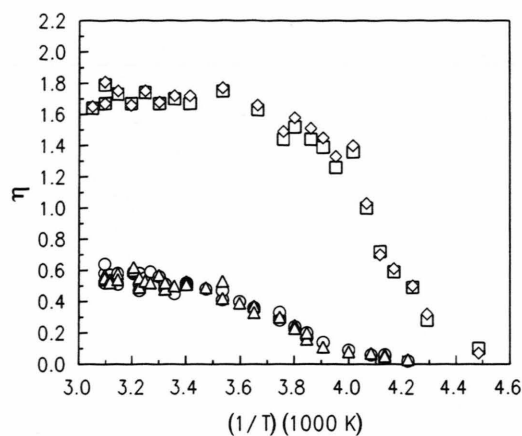
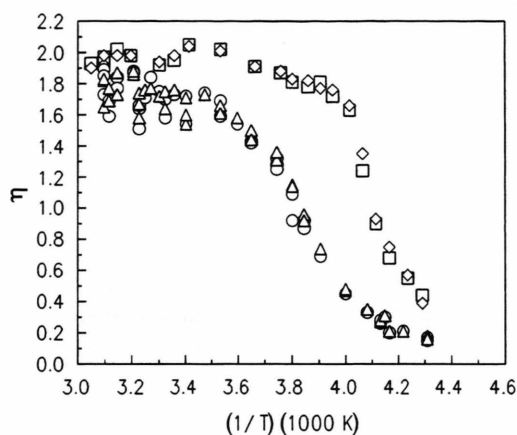
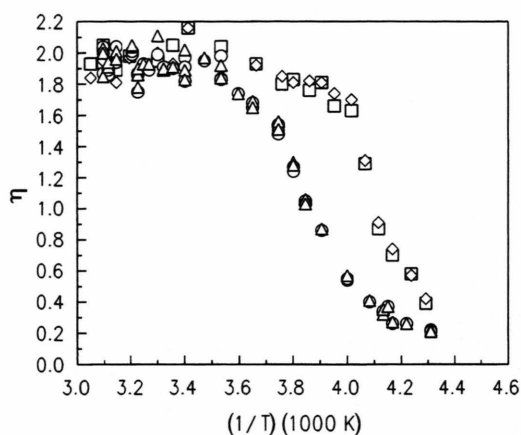
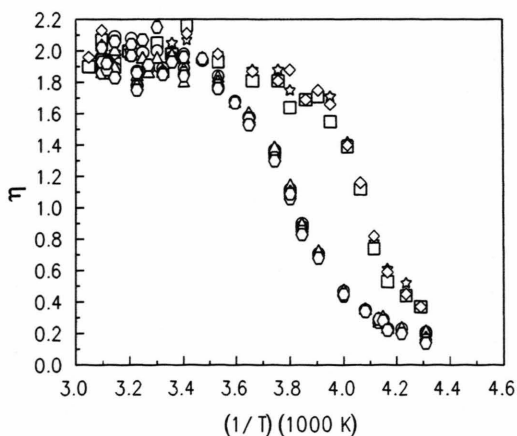
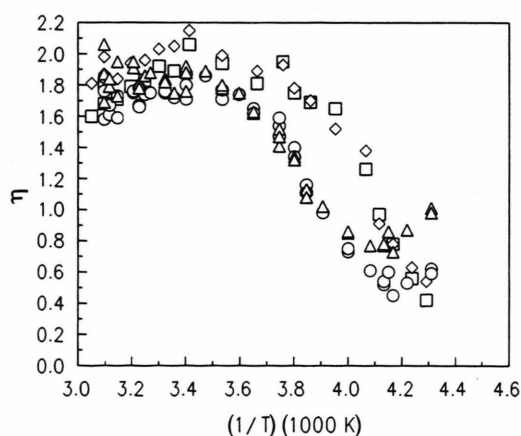
#### 4.2 Parameters of Rotational Motion

The relaxation rates for all  $^{13}\text{C}$  nuclei with directly bonded protons belonging to the rigid molecular frame were very similar when divided by the number

of bonded protons. In the present first approach it was attempted to calculate the observed temperature dependence of the relaxation data to obtain the temperature-dependent rotational motion parameters in a closed analytical form. Representatively for all  $^{13}\text{C}$  nuclei with directly bonded protons, the experimental data of the bridging carbon 9 were fitted with the model parameters introduced in Sect. 2, i.e. (5) to (9) and combinations of them. It turned out that only the spin-lattice relaxation times could be fitted satisfactorily, giving results for which the convergence criterion was fulfilled or for which the standard deviations of the fitted parameters were not too large. Furthermore, a used model is only then capable of describing the experimental data sufficiently when the value of  $\chi^2$  has about the same magnitude as the number of the experimental data points [13]. This criterion was fulfilled only for combinations of the VFT ansatz (8) for the correlation time with either a scaling factor for the dipolar coupling constant (model VFT/C) or with the assumption of a Cole-Davidson distribution (model VFT/CD) of correlation times. These two models were used to fit the experimental longitudinal relaxation times of the remaining carbon atoms except the quaternary carbons for the two measuring frequencies. (In the case of the aromatic methine carbons the experimental rates were fitted without separation of DD and CSA contributions.) For both measuring frequencies the mean value of the parameter  $T_0$  obtained from all carbon atoms with directly bonded protons is quite near to the value of 188 K for the glass transition obtained from DTA data [9]. This was another reason to choose the VFT relation as a starting point for the evaluation.

For the VFT/C approach we chose the distances  $r_{ij}$  as explained in Sect. 2 and the scaling factor in (9) as an adjustable parameter. For the VFT/CD ansatz we set  $C=1$  with the  $r_{ij}$  values as used for the VFT/C approximation and now took  $\beta$  as adjustable parameter instead of  $C$ .

The evaluation of the methyl carbon relaxation needed a special treatment: As already indicated by large  $\chi^2$  values, due to the presence of internal rotation the simple form of (1) or (9) is no longer correct, rather an expression as given by the Woessner formalism [22, 23] or similar ones with two or more terms is needed, depending on the details of molecular motion. At the low measuring frequencies of the present study the separation between the high-temperature maximum and other lower-temperature features of the

A) Quaternary aromatic carbon atoms 4a ( $\square$ ,  $\diamond$ ) and 8a ( $\diamond$ ,  $\Delta$ ).B) Quaternary aromatic carbon atoms 5 ( $\square$ ,  $\diamond$ ) and 6 ( $\diamond$ ,  $\Delta$ ).C) Methine aromatic carbon atoms 7 ( $\square$ ,  $\diamond$ ) and 8 ( $\diamond$ ,  $\Delta$ ).D) Methine aliphatic carbon atoms 1 ( $\square$ ,  $\diamond$ ) and 4 ( $\diamond$ ,  $\Delta$ ).E) Methylene aliphatic carbon atoms 2 ( $\square$ ,  $\diamond$ ), 3 ( $\diamond$ ,  $\Delta$ ), and 9 ( $\star$ ,  $\diamond$ ).F) Methyl carbon atoms 10 ( $\square$ ,  $\diamond$ ) and 11 ( $\diamond$ ,  $\Delta$ ).Fig. 2. Experimental  $^{13}\text{C}$  NOE factors  $\eta$  at 22.63 MHz ( $\square$ ,  $\diamond$ ,  $\star$ ) and 100.62 MHz ( $\diamond$ ,  $\Delta$ ,  $\circ$ ).

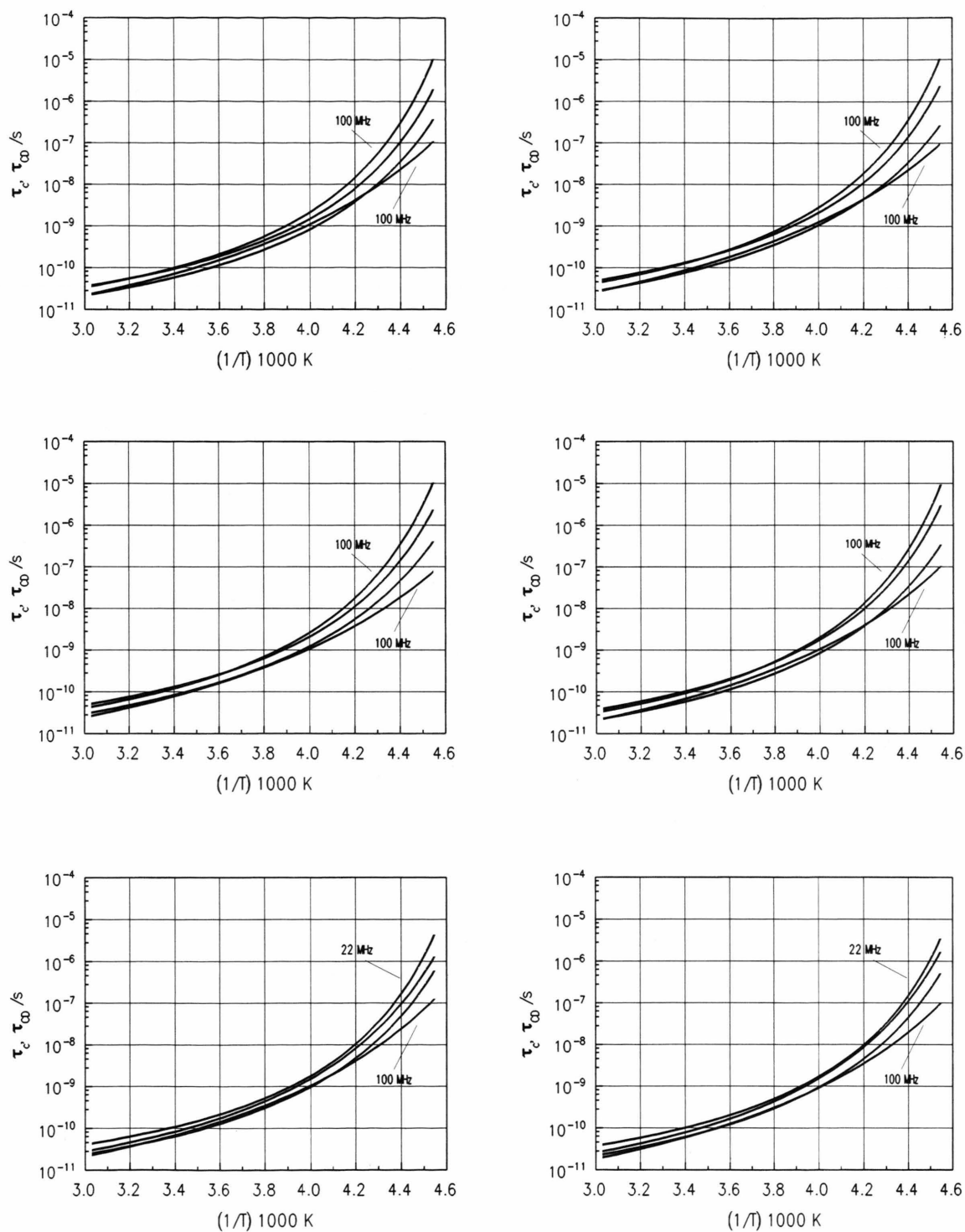
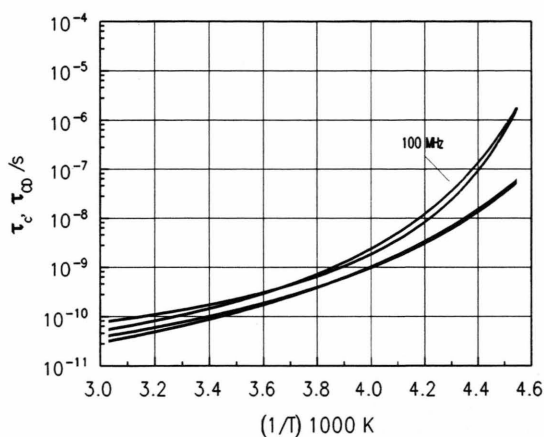
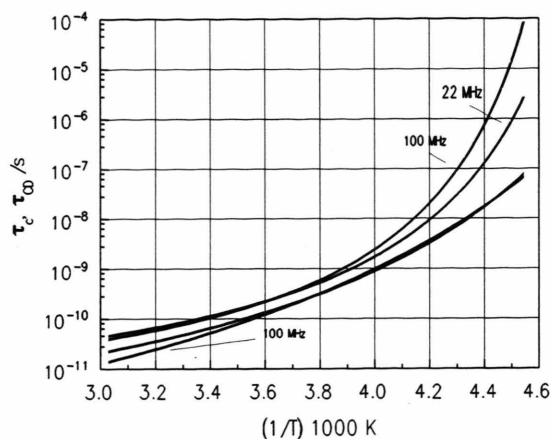
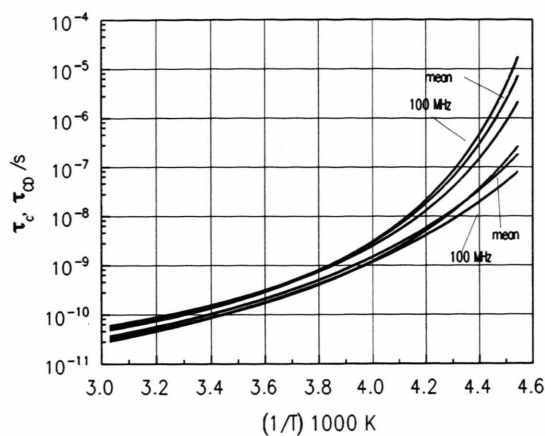


Fig. 3. Correlation times  $\tau_c$  (lower curves) and  $\tau_{CD}$  (upper curves) obtained from the best fit parameters for carbon atoms 1, 2, 3, 4, 7, 8, 9, 10, and 11 (left-hand column top to bottom: C1, 3, 7 next page 9, 11; right-hand column top to bottom: C2, 4, 8, next page 639).





function  $\ln(1/T_1)$ , vs.  $1/T$  is so large that the VFT/C approach still yielded reasonable results. Thus,  $C$  values of about one tenth of those obtained for the other carbons were found. This corresponds approximately to the "Woessner" factor of  $(1/4)(3\cos^2(\theta) - 1)^2 = 0.098$  mentioned above. For the fitting with the VFT/CD model, however, it was necessary to apply an equation which included this geometrical factor in order to obtain reasonable results. Then the resulting dynamic parameters refer to the slow-motion residuum in the fast motion of the methyl  $^{13}\text{C}-^1\text{H}$  vectors, i.e. the reorientational correlation time of the  $\text{C}-\text{CH}_3$  axis. For evaluation of the data at the higher measuring frequency some of the relaxation rates for larger  $1/T$  values have been omitted in the VFT/C and VFT/CD fits in order to avoid the special features of the relaxation curve which are due to additional modes of molecular motion.

The dynamical parameters of carbon atom 9 as representative quantities are collected in Table 1. For the other carbons the dynamical parameters are similar. It can be seen that the numerical values of the respective parameters for one type of  $^{13}\text{C}-^1\text{H}$  vector are not frequency-independent, as, however, must be required. This finding may be interpreted as a consequence of the fact that the validity of the VFT relation (8) was assumed to be true. In particular,  $C$  or  $\beta$  were treated as adjustable parameters, so that even these quantities appear to be frequency-dependent, conflicting with basic requirements of the geometric-dynamical description. The frequency dependence of  $\tau_0$ ,  $E_{\text{VFT}}$ , and  $T_0$  turned out to be smaller for the VFT/CD model than for the VFT/C description. Thus, the former approach should be considered as the better one (but see below). Yet in spite of the variation of parameters the most important quantity is the correlation time  $\tau$  as a function of temperature, which results from the data given in the Table. The corresponding results are given in Fig. 3 which shows that the correlation times of the various  $^{13}\text{C}-^1\text{H}$  vectors are almost equal. However, as to be expected from the representative entries of the Table, they are more or less frequency-dependent, from which again can be concluded that the considered approaches are only approximately valid.

It was not attempted to evaluate the temperature dependence of the spin-lattice relaxation data for the quaternary carbons, since they do not possess directly bonded protons, and it was impossible to calculate proper dipolar spin-lattice relaxation times for them in the extreme narrowing region [10]. Yet the following simple statement can be made: The reorientational

Table 1. Best fit parameters for the Vogel-Fulcher-Tammann models VFT/C and VFT/CD after fitting experimental  $^{13}\text{C}$  spin-lattice relaxation rates of carbon atom 9 in 5,6-Me<sub>2</sub>-THMN.

Distance $^{13}\text{C}-^1\text{H } r_{ij}/\text{pm}$	111.1	
$\nu_0(^{13}\text{C})/\text{MHz}$	22.63	100.62
Number of data points	29	36
StdDev/%	5	3
VFT/C		
$\chi^2$	17	42
$\tau_0/\text{ps}$	1.6	0.60
$E_{\text{VFT}}/\text{kJ mol}^{-1}$	3.7	5.3
$T_0/\text{K}$	183	166
$C$	0.69	0.712
VFT/CD		
$\chi^2$	16	24
$\tau_0/\text{ps}$	3.7	3.1
$E_{\text{VFT}}/\text{kJ mol}^{-1}$	3.2	3.09
$T_0/\text{K}$	191	196.1
$\beta$	0.39	0.462

correlation times for the quaternary  $^{13}\text{C}-^1\text{H}$  vectors are the same as those for the other  $^{13}\text{C}-^1\text{H}$  vectors, because at 22.63 MHz the relaxation function maximum occurs at the same temperature. Furthermore, the relaxation is about 1/15 of that of a  $^{13}\text{C}-^1\text{H}$  pair with a proton directly bonded to the carbon, thus  $n_{\text{H}}/r_{\text{quart}}^6 = (1/15)(1/r_{ij}^6)$ . With  $n_{\text{H}}=6$  a value of about 400 pm is obtained for the dipolar interaction radius  $r_{\text{quart}}$  of the quaternary carbons, which corresponds approximately to the radius of the molecule.

## 5. Discussion

When the VFT ansatz was applied as a starting equation for the description of the temperature dependence of  $\tau$ , only a combination of the VFT relation with either a scaling factor  $C$  for the dipolar coupling constant (model VFT/C) or a Cole-Davidson distribution of the correlation times (model VFT/CD) was appropriate to describe the relaxation data. The CD distribution of correlation times alone could not explain the continuously increasing absolute value of the slope of the relaxation curves. On the contrary, the absolute value of the slope following the maximum (i.e. at larger  $1/T$  values) is generally smaller than before the maximum for a logarithmic plot against reciprocal temperature in case of the CD spectral density. When modeling the data with a VFT ansatz and

the full Lorentzian spectral density, this approach could not account for the comparatively low value of the maximum height.

As can be seen from Fig. 3, the agreement between the correlation times obtained from the fit of the spin-lattice relaxation times for the respective carbon atom with directly bonded protons by the models VFT/C and VFT/CD at the two measuring frequencies is quite satisfactory in the temperature range  $3.0 \leq 1000/T \leq 4.2 \text{ K}^{-1}$ , although in some cases the  $\tau_c$  values are still slightly frequency-dependent. Note that for comparison with the correlation times from the VFT/C model the correlation times derived from the VFT/CD approach in Fig. 3 have to be multiplied by the  $\beta$  values, which then gives the corresponding mean correlation times  $\bar{\tau}_{\text{CD}}$  of the Cole-Davidson correlation time distribution.

In this temperature range the vectors connecting the  $^{13}\text{C}$  nuclei with the directly bonded protons at a given temperature have nearly the same correlation time. This statement includes the slow motion residuum in the fast motion of the methyl  $^{13}\text{C}-^1\text{H}$  vectors. At room temperature ( $T=298 \text{ K}$ ) we find  $\tau_c \approx 6 \cdot 10^{-11} \text{ s}$ . With a molecular radius of 390 pm and a viscosity of 6.43 mPa s the Stokes-Einstein-Debye (SED) formula yields a reorientational correlation time of  $4 \cdot 10^{-10} \text{ s}$ . Generally, the experimental correlation time is smaller than the one obtained from the SED model, a fact which has lead to applying slip boundary conditions instead of stick boundary conditions (cf. [27]). Another aspect, following the point of view in this work, is that a “soft molecule” is considered here (see below). It is obvious that the correlation times must not depend on the measuring frequencies, but above a reciprocal temperature of about  $4.3 \cdot 10^{-3} \text{ K}^{-1}$  the curves in Fig. 3 diverge, what is not surprising since the slope of VFT plots near  $T_0$  increases very fast and a small error in  $T_0$  has large effects on the curve. Furthermore, the relatively small number of spin-lattice relaxation data for 22.63 MHz after the maximum caused difficulties with the fitting procedure.

In order to visualize the quality of the fit for the experimental data, the mean of the fitted parameters for the models VFT/C and VFT/CD at the two frequencies (cf. Fig. 3 G) was used to re-compute the relaxation data for one representative carbon, C9. The results are plotted in Figs. 4 and 5. According to the  $\chi^2$  values the quality of the two models was equal. However, it becomes obvious from Fig. 5 B that the fit

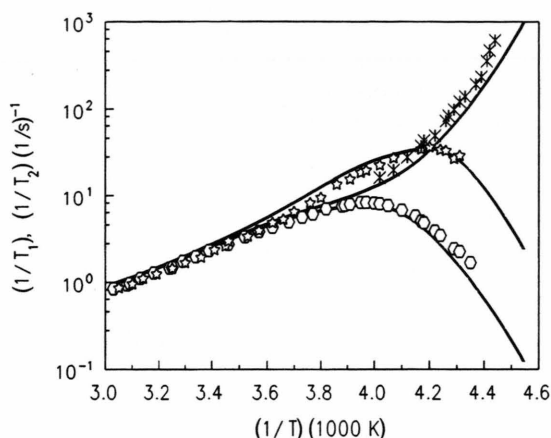


Fig. 4. A) Experimental  $^{13}\text{C}$  longitudinal relaxation rates  $1/T_1$  at 22.63 MHz ( $\star$ ) and 100.62 MHz ( $\circ$ ), transversal relaxation rates  $1/T_2$  at 100.62 MHz ( $\ast$ ), and relaxation data calculated by the mean values of the best fit parameters of the VFT/C model (—) for carbon atom 9.

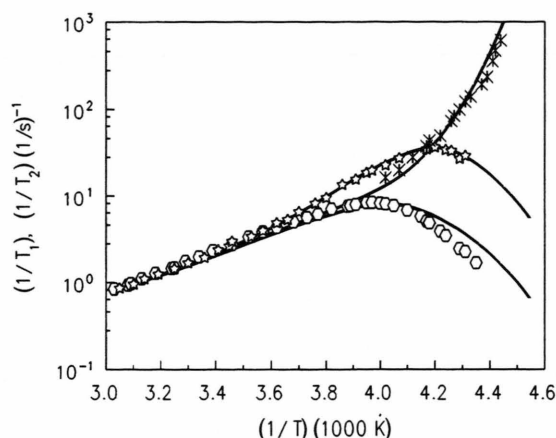


Fig. 5. A) Analogous to Fig. 4 A, relaxation data calculated by the mean values of the best fit parameters of the VFT/CD model (—).

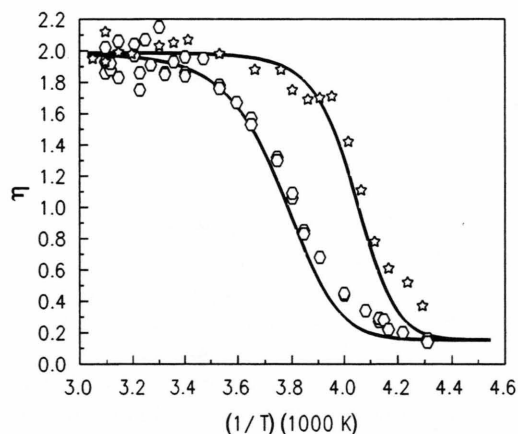


Fig. 4. B) Experimental  $^{13}\text{C}$  NOE factors  $\eta$  at 22.63 MHz ( $\star$ ) and 100.62 MHz ( $\circ$ ), and NOE factors calculated by the mean values of the best fit parameters of the VFT/C model (—) for carbon atom 9.

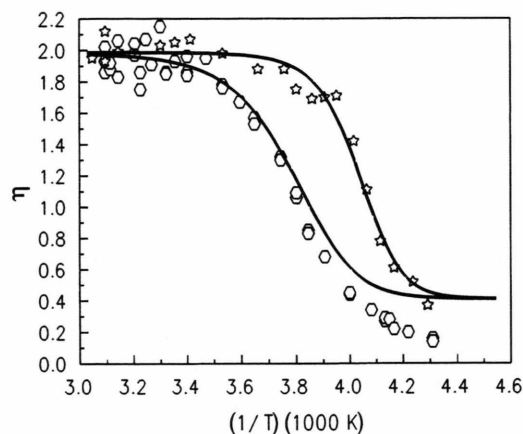


Fig. 5. B) Analogous to Fig. 4 B, NOE factors calculated by the mean values of the best fit parameters of the VFT/CD model (—).

of the NOE factors by the VFT/CD model is not satisfactory at low temperatures. The limiting value of  $\eta_{\max}$  for large  $\omega\tau$  is 0.154 when in (4) Lorentzian spectral densities are introduced. Thus, although the dynamical parameters obtained for the VFT/CD model from fitting the experimental spin-lattice data are less frequency-dependent, the NOE factors show that the combination of the VFT ansatz with the CD correlation time distribution function is less acceptable as an explanation for the presented experimental data.

The spin-lattice relaxation rate maximum was found to be diminished by a factor  $C=0.70$ . One explanation of this fact could be a lowering of the dipolar coupling constant which is proportional to the C–H distance with  $r_{\text{C-H}}^{-6}$ . The value of  $C$  would correspond to an increase of the C–H distance by approximately 6% from 111 to 118 pm. However, such an increase of the bond distance cannot be justified. The remaining explanation for the missing spectral density is a motion which is not considered by the applied

models for evaluation of the relaxation data. Thus, the rigidity condition [1, 2] is not fulfilled. Such a system of bound atoms was called a "soft molecule" in previous publications of one of the authors [3, 4]. Yet it is surprising that all  $^{13}\text{C}$ – $^1\text{H}$  vector correlation times including the slow motion residua of the methyl  $^{13}\text{C}$ – $^1\text{H}$  vectors are virtually the same.

## 6. Conclusions

The recently published results concerning the rotational dynamics of the hydrocarbon 5,6-Me<sub>2</sub>-THMN (**1**) were obtained from  $^{13}\text{C}$  relaxation data in the extreme narrowing region [10]. They lead to the conclusion that the rotational behavior of **1** is well described by the model of rotational diffusion of rigid bodies. In the present study also data from outside the extreme narrowing regime were considered. The results demonstrate clearly that the model of rigid bodies does not account for the missing spectral density. The model which could reproduce the experimental data had the effect of apparently diminishing the dipole

lar coupling constant by a factor of 0.70 for all carbon atoms with directly bonded protons. Admittedly, the scaling factor *C* does not play any role for the calculation of the NOE factors because it cancels out. Possibly, the truth is given by an intermediate approach: There is a Cole-Davidson distribution of correlation times present and a certain amount of "concealed" very high-frequency motion. Then the simple analytical representation of the temperature dependence for the correlation times in the form of the VFT relation has to be given up or at least modified. The authors are at present examining this possibility further. In consequence, the presented analysis has to be regarded as preliminary.

## Acknowledgements

Financial support by the Deutsche Forschungsgemeinschaft (Do 363/1-1) and Fonds der Chemischen Industrie (A.D.) is gratefully acknowledged. The authors thank P. Gruhlke for providing them with the viscosity data.

- [1] H. G. Hertz, *Progr. NMR Spectrosc.* **16**, 115 (1983).
- [2] H. G. Hertz, *Lect. Notes Phys.* **293**, 41 (1987).
- [3] M. Pöschl and H. G. Hertz, *J. Phys. Chem.* **98**, 8181 (1994).
- [4] M. Pöschl and H. G. Hertz, *J. Phys. Chem.* **98**, 8195 (1994).
- [5] M. D. Zeidler, *Ber. Bunsenges. Phys. Chem.* **95**, 972 (1991).
- [6] D. W. Davidson and R. H. Cole, *J. Chem. Phys.* **19**, 1484 (1951).
- [7] W. Müller-Warmuth and W. Otte, *J. Chem. Phys.* **72**, 1749 (1980).
- [8] A. Dölle and T. Bluhm, *J. Chem. Soc., Perkin Trans. 2* **1985**, 1785.
- [9] J. Reuter, T. Brückert, and A. Würflinger, *Z. Naturforsch.* **48a**, 705 (1993).
- [10] A. Dölle and T. Bluhm, *Mol. Phys.* **59**, 721 (1986).
- [11] M. Pöschl, G. Althoff, S. Killie, E. Wenning, and H. G. Hertz, *Ber. Bunsenges. Phys. Chem.* **95**, 1084 (1991).
- [12] A. L. Van Geet, *Anal. Chem.* **40**, 2227 (1968).
- [13] W. H. Press, B. P. Flannery, S. A. Teukolsky, and W. T. Vetterling, *Numerical Recipes. The Art of Scientific Computing*, Cambridge University Press, Cambridge 1989.
- [14] M. J. S. Dewar, E. G. Zoebisch, E. F. Healy, and J. J. P. Stewart, *J. Am. Chem. Soc.* **107**, 3902 (1985).
- [15] MOPAC, IBM Version 5.01, QCPE 581.
- [16] J. R. Lyerla and G. C. Levy, *Top. Carbon-13 NMR Spectrosc.* **1**, 79 (1972).
- [17] D. Neuhaus and M. Williamson, *The Nuclear Overhauser Effect in Structural and Conformational Analysis*, VCH Publishers, New York 1989.
- [18] H. Vogel, *Phys. Z.* **22**, 645 (1921).
- [19] G. Fulcher, *J. Amer. Ceramic Soc.* **8**, 339 (1925).
- [20] G. Tammann and W. Hesse, *Z. Anorg. Allg. Chem.* **156**, 245 (1926).
- [21] U. Schlenz, *Dissertation, Universität Karlsruhe, Karlsruhe* 1992.
- [22] D. E. Woessner, *J. Chem. Phys.* **36**, 1 (1962).
- [23] D. E. Woessner, *J. Chem. Phys.* **37**, 647 (1962).
- [24] M. S. Ansari and H. G. Hertz, *Z. Phys. Chem.* **146**, 15 (1985).
- [25] H. Versmold, *Ber. Bunsenges. Phys. Chem.* **78**, 1318 (1974).
- [26] H. Versmold, *Nuclear Magnetic Relaxation and Molecular Reorientation*, In: A. J. Barnes, W. J. Orville-Thomas, and J. Yarwood (eds.): *Molecular Liquids. Dynamics and Interactions*, D. Reidel Publishing Company, Dordrecht, 1984.
- [27] D. Kivelson, *Lect. Notes Phys.* **293**, 1 (1987).